RAPID COMMUNICATIONS

PHYSICAL REVIEW E VOLUME 52, NUMBER 2 AUGUST 1995

Internal surface, orientational order, and distribution of a polymer network in a liquid crystal matrix

G. P. Crawford,[1] A. Scharkowski,[1] Y. K. Fung,[1] J. W. Doane,[1] and S. Zumer[1,2]
[1]*Liquid Crystal Institute, Kent State University, Kent, Ohio 44242-0001*
[2]*Department of Physics, University of Ljubljana, Jadranska 19, 61000 Ljubljana, Slovenia*
(Received 12 December 1994)

Optical birefringence of the liquid crystal induced in its isotropic phase by low concentration polymer networks (1–4 % by weight) is used to estimate the internal surface area of the network and its order parameter. The results show conclusively that the polymer networks are finely distributed down to the nanometer scale with the orientational order parameter being an order of magnitude smaller than that of the nematic medium where they are formed. A model structure is presented where molecular fibrils form bundles (relatively rich in polymer) which are responsible for the observed inhomogeneities on the submicrometer scale.

PACS number(s): 61.30.Gd, 61.41.+e

Polymer networks formed within an anisotropic liquid crystal environment, explored by Mariani and co-workers [1], have recently been exploited for many electro-optic applications from a bistable reflective display [2] to a controlled scattering light shutter [3]. These very low concentration polymer networks capture the image of the orientational order of the original liquid crystal medium indefinitely [4]. Such dispersions are complex soft matter systems with physical properties analogous to liquid crystals confined to well defined submicrometer cavities [5–7] and random porous systems [8–11] which are currently attracting a lot of attention. The first clues into the structures of these polymer networks were deduced from electron microscopy [1,12], birefringence [12,13], dichroism [12], and dielectric response [14] in systems with high network concentration, and from magnetic resonance [15], diamagnetic and viscosity [16], and small angle neutron scattering [17] measurements. Open questions concerning the distribution of the polymer network in space, particularly in the low concentration case, stimulated us to perform an optical birefringence study of networks polymerized in a nematic director field stable in supramicrometer capillary tubes.

Samples are prepared by dissolving 1–4 wt % of diacrylate monomer 4,4′-bis-acryloylbiphenyl (BAB) and ~0.5 wt % of the photoinitiator benzoin methyl ether (BME) into the nematic liquid crystal 4′-pentyl-4-cyanobiphenyl (5CB). The nematic-isotropic (N-I) transition temperature $T_{N\text{-}I}$ of bulk 5CB is 34.9 °C. The sample was homogenized at 100 °C, filled into lecithin treated capillary tubes (radii: $R=50$–450 μm) at ambient temperature, and immersed in glycerin to minimize refraction for optical studies [18]. Prior to photopolymerization the nematic director fields in the capillary tubes were radial at the surface and exhibited escape in the axial direction in the central part of the tubes [6,19]. After photopolymerization, the polymer network captures the image of the director field. The optical (white light) polarization microscope textures [Figs. 1(a) and 1(c)] recorded above the N-I transition reveal that the images are permanently locked-in even at temperatures deep in the isotropic phase [see Figs. 1(a) and 1(c)]. With a strong electric field (electric coherence length [20] ≪diameter of the capillary) perpendicular to the cylinder axis, a homogeneous director field along the electric field direction was stabilized [Fig. 1(e)] [21]. The samples were polymerized by uv radiation (high pressure mercury lamp 24 mW/cm^2) at ambient temperatures for ~40 min. Samples for scanning electron microscopy (SEM) observations were prepared in lecithin treated planar cells which enforce normal surface anchoring. After photopolymerization, the samples were carefully opened and the liquid crystal was subsequently evaporated off, leaving behind only the polymer network.

A study of the nematic ($T<T_{N\text{-}I}$) birefringent texture shows a significant increase in light scattering after polymerization, indicating that some structures on the scale of the wavelength of light are formed. The submicrometer size inhomogeneities are clearly visible from SEM images (see Fig. 2); therefore it is difficult to optically study the structure of the network in the nematic phase because of strong scattering. At temperatures above $T_{N\text{-}I}$, an optical anisotropy remains but its value is significantly reduced such that the effects of light scattering are minimized. The interference colors observed with white light in a cylinder with $R=150$ μm indicate low birefringence (difference between extraordinary and ordinary index of refraction) $\Delta n_{\text{pilc}}\sim 10^{-3}$, where the subscript pilc denotes polymer in liquid crystal.

To measure Δn_{pilc}, we calculate the interference patterns for a cylindrical tube between crossed polarizers [18] with a homogeneously aligned director field $\mathbf{n}$ [Fig. 1(e)]. The intensity of the transmitted light with wavelength λ polarized at 45° with respect to the plane defined by the director field $\mathbf{n}$ (optical axis) and the incoming light direction $\mathbf{k}$ is given by $I=I_0\sin^2(\delta/2)$. Here $\delta=4\pi(R^2-r^2)^{1/2}\Delta n_{\text{pilc}}\sin^2\beta/\lambda$ is the phase shift between the ordinary and extraordinary component of light, r the distance from the symmetry plane of the capillary, and β the angle between vectors $\mathbf{k}$ and $\mathbf{n}$ [Fig. 1(e)]. The values of Δn_{pilc} (see Fig. 3) were determined for various polymer concentrations c and temperatures by fitting the experimental intensity distribution $I(r)$ [18].

The pretransitional increase of the otherwise small birefringence (Fig. 3) suggests that beside the contribution to Δn_{pilc} arising from the partially ordered polymer network, there is also a contribution from the paranematic order induced in the isotropic liquid crystal by the internal surfaces

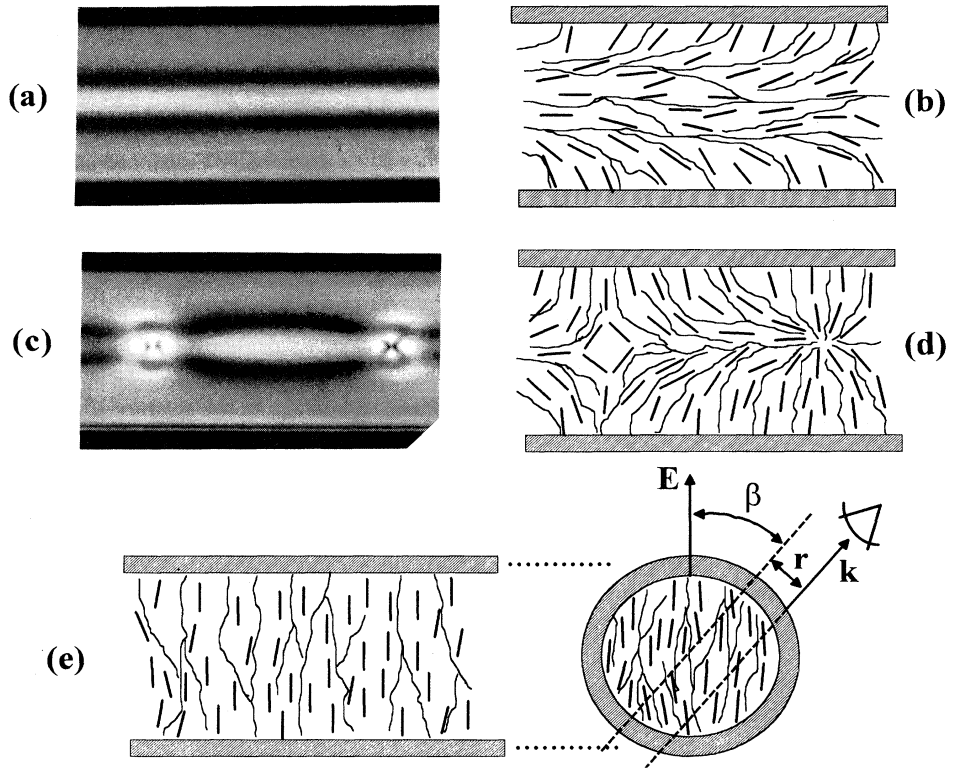

FIG. 1. The optical birefringence patterns of the nematic director field images captured in the 4% polymer network obtained by first polymerizing in the nematic phase then heating the sample to the isotropic phase (25 K above the $T_{N\text{-}I}$) and photographed with white light under crossed polarizers (a) and (c). The system corresponding to pattern (a) was formed in a radial director field with an axial escape in the central area of the cylinder and is schematically presented in (b). The pattern (c) shows point defects that were captured during photopolymerization; they are schematically presented in (d). The defects can exist because both directions of bend are energetically equivalent and oppose one another [6,19]. The schematic presentation (e) shows the field aligned director configuration with the goemetry for the determination of the birefringence.

of the network. To separate these contributions, we substitute the liquid crystal which surrounds the network with the isotropic fluid chlorobenzene. Using the above method, the effective birefringence Δn_{pil} (the subscript pil denotes polymer in liquid) for the network in chlorobenzene was estimated to be between 3 to 8×10^{-4} depending on the network concentration but independent of temperature up to 130 °C (Fig. 3).

We conclude that the substitution of the liquid crystal with chlorobenzene does not effect the partially ordered network, since there are no appreciable changes in the volume occu-

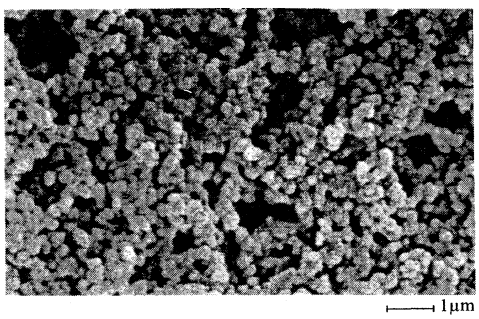

FIG. 2. Scanning electron microscopy image of a dried polymer network indicates inhomogeneity on the submicrometer scale.

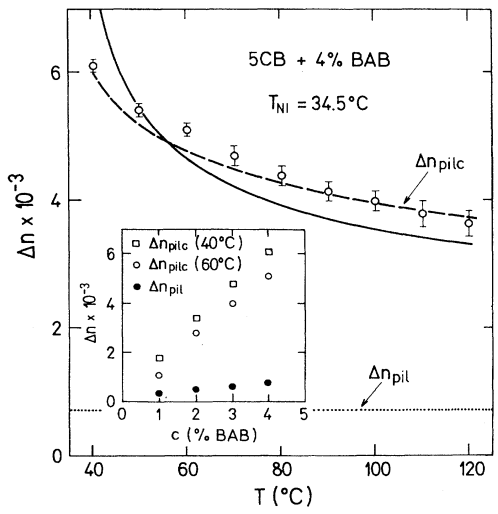

FIG. 3. The optical birefringence of the polymer-liquid crystal (Δn_{pilc}) and polymer-isotropic liquid (Δn_{pil}) dispersions for a light with $\lambda = 589$ nm as a function of temperature and concentration of polymer (inset). The solid line shows the fit to Eq. (2) for the one parameter model (uniform distribution of fibrils) and the broken line is the fit to the two parameter model (bundles of fibrils).

pied by the network and the images of the nematic director field stored in the network are preserved. The birefringence can be attributed only to the network because chlorobenzene molecules are too spherical to expect ordering. In composite systems where differences in dielectric constants are small and the network distribution is inhomogeneous on the subwavelength scale, the effective birefringence $\Delta n_{\rm pil}$ is expected to be well described by the spatial average $cQ_p\Delta n_{\rm op}$, when factors on the order of 1 are neglected. Here c is the network concentration, $\Delta n_{\rm op}$ is the birefringence of the completely oriented network, and Q_p is the spatial average of the order parameter of the network. Using the experimental values of $\Delta n_{\rm pil}$ and c, and assuming that $\Delta n_{\rm op}$ of the oriented polymer is comparable to $\Delta n_0 \sim 0.35$ [22] of the completely oriented liquid crystal (because of the chemical similarity between 5CB and BAB), one finds Q_p between 0.08 and 0.05. This is approximately 5 to 8 times smaller than in the original liquid crystal environment where it was formed, which indicates a substantial amount of the cross linking. It is also much less than reported in the more concentrated diacrylate networks [12]. Without additional experiments, we cannot determine how much order is local and how much occurs on larger scales. When the network is surrounded by the isotropic liquid crystal, the birefringence $\Delta n_{\rm pilc}$ includes a contribution from the ordering of the liquid crystal molecules induced by the internal surfaces of the polymer along the ordering direction of the network. In the same approximation as above one can write

$$\Delta n_{\rm pilc} = \Delta n_0 \left(cQ_p + \int_V Q(\mathbf{r}) dV/V \right). \quad (1)$$

Here $Q(\mathbf{r})$ is the induced spatial dependence of the orientational order parameter of the liquid crystal and V is the volume of the system. Instead of following the two fraction model used in Ref. [23] that cannot describe the pretransitional phenomena, we use the results for $Q(\mathbf{r})$ obtained in our studies of surface induced ordering in liquid crystals confined to small cavities [7,24]. The spatial dependence of the surface induced orientational order is described simply as constant order Q_0 in the first molecular layer of thickness ξ_m for distances from the surface $z > \xi_m$ followed by a decay described by the Landau–de Gennes theory. To solve the integral in Eq. (1) in a simple analytic form, we neglect the details of the geometry and use the results for weak anchoring in a planar geometry: $Q = Q_0 \exp[(\xi_m - z)/\xi]$ for $z > \xi_m$. Here the nematic correlation length is given by $\xi = \xi_0 (T/T^* - 1)^{-1/2}$ with $\xi_0 = 0.65$ nm and $T^* = 306$ K for 5CB [25]. The results will only be qualitative when the surface is not planar on the scale ξ. A relatively weak temperature dependence of $\Delta n_{\rm pilc}$ according to our study of surface induced ordering in cavities [7] where a similar situation was realized for planar anchoring [7] indicates that the coupling between polymer surface and liquid crystal is strong. We therefore assume that the coupling enforces the surface order parameter of liquid crystal to be equal to the order parameter of the network in the entire temperature range. Because we are interested in the average values we simply take $Q_0 = Q_p$. Equation (1) can thus be written as

$$\Delta n_{\rm pilc} \cong \Delta n_{\rm pil} + \Delta n_0 Q_0 (\xi_m + \xi) A/V \quad \text{with} \quad \Delta n_{\rm pil} = Q_0 \Delta n_0 c. \quad (2)$$

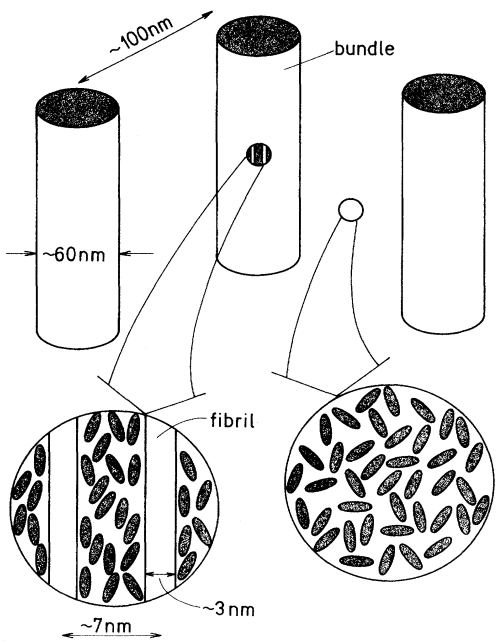

FIG. 4. Schematic presentation of our model structure of the polymer network in a liquid crystal solvent showing bundles distributed on the submicrometer level and molecular fibrils on the nonometer scale. Intentionally no cross linking is shown.

Here A is the effective internal surface areas of the network which introduces paranematic ordering in the isotropic liquid crystal. We estimate the internal surface area per unit volume of the polymer network, $\alpha = A/cV \sim (1 \pm 0.5)$ nm^{-1}, from a single parameter fit of experimental $\Delta n_{\rm pilc}$ to the expression $\Delta n_{\rm pil}[1 + (\xi_m + \xi)\alpha]$ (Fig. 3). To envision how finely the polymer network is distributed in the liquid crystal let us use two simplified models: a regular square array of parallel cylindrical fibrils [16] with radius R and interfibril distance b, and a square lattice of polymer sheets [23] with thickness t and intersheet distance L. For the fibril model, the internal surface area per volume is $\alpha = 2/R$ and the concentration is $c = \pi R^2/b^2$; therefore we estimate the radius $R \sim 2$ nm and interfibril distance b between 16 and 34 nm as c goes from 4% to 1%. For the sheet model, $\alpha = 1/t$ and $c = 2t/L$; therefore we obtain $t = 1$ nm and the lattice distance L between 50 and 200 nm depending on c. Because of the symmetry of the initial nematic environment where the network is formed, the actual structure is probably closer to the fibril model but with a lot of interconnections. Cross linking is responsible for low average order parameters and high stability of the polymer network.

These results are apparently in contradiction with enhanced light scattering caused by the network in the nematic phase and scanning electron microscopy images (Fig. 3) which both indicate structures on the larger submicrometer scale. In addition, recent small angle neutron scattering measurements [17] indicate that the mean diameter of the network fibers is 50–60 nm not depending much on the polymer concentration. This information can be consistently explained by introducing the inhomogeneities in the distribution of our thin molecular fibrils. We propose the following model (see Fig. 4): molecular fibrils with nanometer size

radii R form bundles (fibers) of polymer rich material separated by a liquid crystal background (polymer poor material). In the bundles with a diameter of 60 nm, the network strongly influences the liquid crystal, even in the isotropic phase (paranematic ordering). The interfibril distance $b \sim \xi$ indicates that a saturation of the network ordering effect must be expected. In evaluating the integral in Eq. (1), this is approximately taken into account by reducing the integration range of the order parameter decay to b yielding a substitution of ξ in Eq. (2) by $\xi\{1-\exp[(\xi_m-b)/\xi]\}$. A much better two parameter fit of our 4% data yields a 20% larger α with $R \sim 1.5$ nm and $b \sim 7$ nm (Fig. 3). For 4% polymer concentrations this value of the interfibril distance corresponds to an average distance between bundles of about 100 nm. In the isotropic phase the liquid crystal molecules in between bundles is thus not effected by the network. In the nematic phase, however, the constraints on the liquid crystal exhibited by the bundles are relatively strong and are the basis for electro-optic applications in these systems [2,3].

We can conclude that we have succeeded to estimate the effective internal surface of the low concentration network polymerized in a nematic liquid crystal matrix. It should be emphasized that this large internal surface area per unit volume of the polymer predicted by all our model structures leads to the same conclusion: at least one dimension of the network is comparable to typical molecular size. In agreement with all available experimental facts, we further propose a model structure where molecular fibrils ($R \sim 1.5$ nm) form bundles rich in polymer which are responsible for the inhomogeneities on the submicrometer scale. To improve our model, more detailed optical birefringence experiments and refinement of the theoretical description similar to the one developed for random spin systems [11] are planned.

This research was supported in part by the National Science Foundation (NSF) Science and Technology Center ALCOM DMR89-20147. The authors gratefully acknowledge discussions with Dr. Dengke Yang and Dr. L.-C. Chien.

[1] P. Mariani, B. Samori, A. S. Angeloni, and P. Ferruti, Liq. Cryst. **1**, 327 (1986).

[2] D. K. Yang, L.-C. Chien, and J. W. Doane (unpublished); D. K. Yang, L.-C. Chien, and J. W. Doane, Appl. Phys. Lett. **60**, 3102 (1992).

[3] R. A. M. Hikmet, Mol. Cryst. Liq. Cryst. **213**, 117 (1992).

[4] G. P. Crawford, R. D. Polak, A. Scharkowski, L. C. Chein, S. Zumer, and J. W. Doane, J. Appl. Phys. **75**, 1968 (1994).

[5] J. H. Erdman, S. Zumer, and J. W. Doane, Phys. Rev. Lett. **64**, 1907 (1990).

[6] D. W. Allender, G. P. Crawford, and J. W. Doane, Phys. Rev. Lett. **67**, 1442 (1991); R. D. Polak, G. P. Crawford, B. C. Kostival, J. W. Doane, and S. Zumer, Phys. Rev. E **49**, R978 (1994).

[7] G. P. Crawford, R. J. Ondris-Crawford, S. Zumer, and J. W. Doane, Phys. Rev. Lett. **70**, 1838 (1993).

[8] T. Bellini, N. A. Clark, C. Muzny, L. Wu, C. W. Garland, D. W. Schaefer, and B. J. Oliver, Phys. Rev. Lett. **69**, 788 (1992); N. A. Clark, T. Bellini, R. M. Malzbender, B. N. Thomas, A. G. Rappaport, C. D. Muzny, D. W. Schaefer, and L. Hrubest, Phys. Rev. Lett. **71**, 3505 (1993).

[9] X-l. Wu, W. I. Goldburg, M. X. Liu, and J. Z. Xue, Phys. Rev. Lett. **69**, 470 (1992).

[10] G. S. Iannacchione, G. P. Crawford, S. Zumer, J. W. Doane, and D. Finotello, Phys. Rev. Lett. **71**, 2595 (1993).

[11] A. Maritan, M. Cieplak, T. Bellini, and J. R. Banavar, Phys. Rev. Lett. **72**, 4113 (1994).

[12] R. A. M. Hikmet, Liq. Cryst. **9**, 405 (1991). 1991

[13] R. A. M. Hikmet, J. Appl. Phys. **68**, 4406 (1990).

[14] R. A. M. Hikmet and B. H. Zwerver, Liq. Cryst. **10**, 835 (1991).

[15] R. Stannarius, G. P. Crawford, L.-C. Chien, and J. W. Doane, J. Appl. Phys. **70**, 135 (1991).

[16] A. Jakli, D. Kim, L.-C. Chien, and A. Saupe, J. Appl. Phys. **72**, 3161 (1992).

[17] A. Jakli, L. Bata, K. Fodor-Csorba, L. Rosta, and L. Noirez, Liq. Cryst. **17**, 227 (1994).

[18] A. Scharkowski, G. P. Crawford, S. Zumer, and J. W. Doane, J. Appl. Phys. **73**, 7280 (1993).

[19] P. E. Cladis and M. Kleman, J. Phys. (Paris) **33**, 591 (1972).

[20] P. G. deGennes and J. Prost, *The Physics of Liquid Crystals* (Clarendon, Oxford, 1993).

[21] S. Kralj and S. Zumer, Liq. Cryst. **15**, 521 (1993).

[22] R. G. Horn, J. Phys. (Paris) **39**, 105 (1978).

[23] R. A. M. Hikmet and R. Howard, Phys. Rev. E **48**, 2752 (1993).

[24] G. P. Crawford, D. K. Yang, S. Zumer, D. Finotello, and J. W. Doane, Phys. Rev. Lett. **66**, 723 (1991).

[25] H. J. Coles, Mol. Cryst. Liq. Cryst. **49**, 67 (1978).

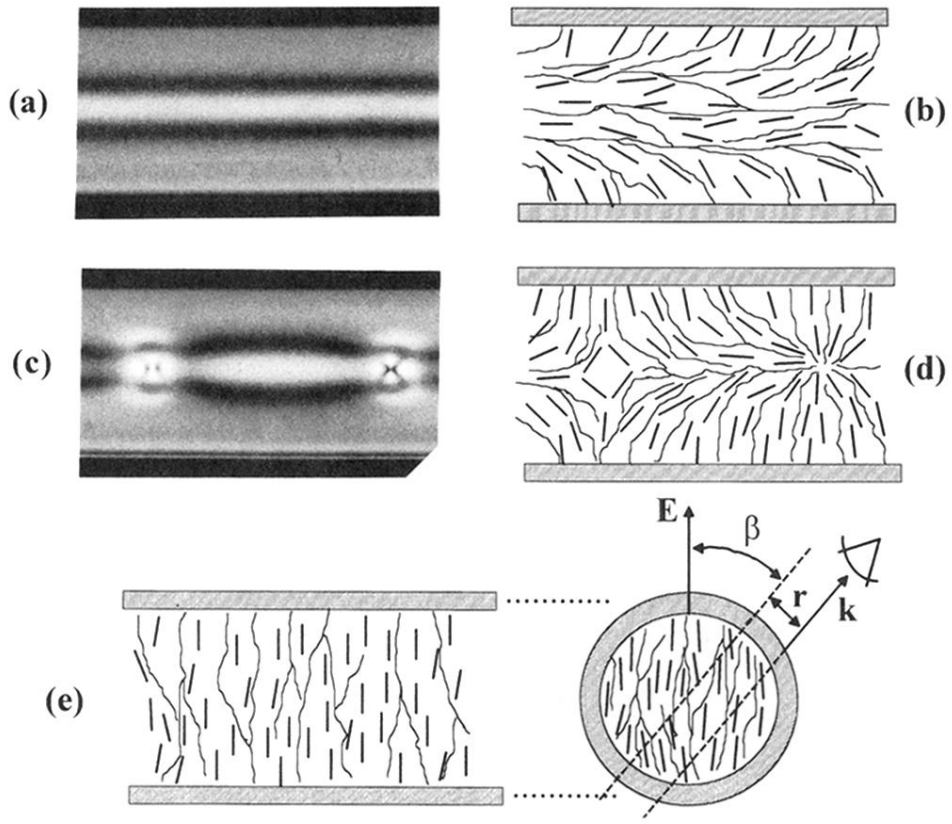

FIG. 1. The optical birefringence patterns of the nematic director field images captured in the 4% polymer network obtained by first polymerizing in the nematic phase then heating the sample to the isotropic phase (25 K above the $T_{N\text{-}I}$) and photographed with white light under crossed polarizers (a) and (c). The system corresponding to pattern (a) was formed in a radial director field with an axial escape in the central area of the cylinder and is schematically presented in (b). The pattern (c) shows point defects that were captured during photopolymerization; they are schematically presented in (d). The defects can exist because both directions of bend are energetically equivalent and oppose one another [6,19]. The schematic presentation (e) shows the field aligned director configuration with the goemetry for the determination of the birefringence.

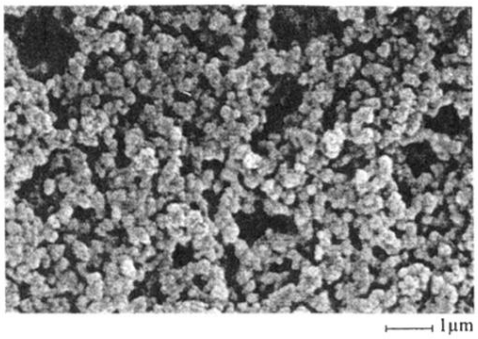

FIG. 2. Scanning electron microscopy image of a dried polymer network indicates inhomogeneity on the submicrometer scale.